COOLING EFFECTS ON BOUNDARY LAYER GROWTH AND HEAT TRANSFER IN GAS TURBINE BLADING CASCADE

H. A. Abdalla, M. Khalil Bassiouny, T. I. Sabry and Mostafa A. Abdel-Baky

Department of Mechanical Power Engineering, Faculty of Engineering, Minufiya University, Shebin El-Kom, Egypt.

ABSTRACT

In this paper, the effect of internal cooling of gas turbine blades has been investigated experimentally. The experiments were performed with seven blades linear cascade of first stage gas turbine. The test results involve the distributions of static pressure and temperature on both pressure and suction blade surfaces as well as the velocity profiles. The boundary layer parameters, the heat transfer coefficient and blade cooling effectiveness in case of variable surface temperature distributions were estimated for different inlet conditions and different coolant mass flow rates. The experimental data were obtained for three cases; cold air, hot gas flow without cooling of the blade and hot gas flow with blade cooling. The results have indicated that, the heat transfer coefficient is decreased while the cooling effectiveness is increased when the coolant air temperature decreases. The cooling of blades causes an increase of the boundary layer parameters compared to uncooled blades. The location of cooling passage near the leading edge affects the boundary layer transition and increases the thickness of the boundary layer and this in turn causes a more reduction in the heat transfer coefficient.

Keywords: Gas turbine, Internal cooling, Blade cooling effectiveness.

INTRODUCTION

Modern design of gas turbine plants and turbojet engines is concerned with the improvement of thermal efficiency and specific output. This improvement of plant efficiency necessitate inlet gas temperature as high as possible. Typical values of turbine entry temperature in modern aero-engines are about 1500 K. Gas turbines which are at present used for long life duties either in aero-propulsion or marine propulsion are limited to gas temperature of order of 1000-1200 K at its entry. Higher temperature results in a deterioration of material strength and creep properties which impose limits on the allowable stress and operating life. Thus, turbine hot flow pass components must be cooled in order to be able to operate in the high gas temperature environment to which they are exposed in modern high performance engines. The cooling methods used in advanced gas turbine applications using high pressure bleed air, are impingement cooling, convective cooling, transpiration cooling, trailing edge bleed and discrete hole film cooling. Convection cooling is the most widely used method of blade cooling.

Cooling is generally accomplished by means of a system using compressor bleed air. The cooling system must be designed to ensure that maximum component temperature and temperature gradients experienced during engine operation are compatible with the maximum stress limits imposed by cycle life, stress rupture and creep for the design operating life of components. Additionally, since the use of compressed bleed air for cooling partially offsets the performance improvement due to

the high turbine inlet temperature, the amount of cooling air used must be minimized to achieve the maximum benefits of the high cycle temperature. To illustrate the importance of minimizing cooling air consumption, it may be noted that each one percent of compressor discharge air used for cooling causes about 0.75 percent increase in the specific fuel consumption of a typical high bypass, high pressure ratio turbofan engines, [1,2].

Initial investigations into the cooling of gas turbines were of an analytical nature and were directed at determining methods and effectiveness of cooling solid turbine blades [3]. The addition of fins to blade tips and rotor, the use of cooling and the use of ceramic coatings on solid turbine blades were investigated [4]. The possibility of using ceramic turbine blades was also considered in Reference 5. When it was found that these schemes would not withstand the temperature increases contemplated and that ceramic blades would not withstand the shock imposed in them. Analytical investigations of temperature distributions through both air and liquid cooled turbine blades were made in Reference 6. Hannis and Smith [7] designed and tested a cooled first stage for an industrial gas turbine to measure the performance of the cooled blades. They indicated an improvement of the gas turbine performance with blade cooling. Kennon and Dulicravich [8] developed a procedure for the efficient design and analysis of coolant flow passage shapes in internally cooled configurations. The method was particularly applicable to turbine blade design but can also be used for the design of other configurations that utilize internal or external cooling such as missile cone tips, rocket nozzles and internal combustion chamber. The method is not limited to cascade design but can also be used for the fully three dimensional design of coolant flow passages.

Heat transfer rate between the hot gas flow and turbine blades strongly affects the life of turbine blades. Daniels and Brown [9] studied the heat transfer rate to gas turbine blades for two inlet mass flow rates at constant wall and stagnation temperatures. The wall heat flux measurement technique allowed the test result to be expressed in terms of an isothermal wall. Walker and Markland [10], in their experiments to measure the local heat transfer coefficients of turbine blading in the presence of secondary flow around chord-wise profiles of one blade of a cascade, used an electrical heater to heat the blade to a few degrees above the air stream temperature. They concluded that the heat transfer coefficient may be increased by changing the total pressure along the blade span due to the variation of the boundary layer transition with respect to the blade leading edge. Kapinos and Sletenko [11] have reported a correlation formula for determining the average heat transfer coefficient. The formula takes into account the geometrical parameters of the cascade but did not involve the effect of blade cooling on the heat transfer coefficient.

The end wall heat transfer and aerodynamics in a linear blade cascade was investigated experimentally by York *et. al.* [12] under conditions that simulate those in first stage stator of an advanced turbine engines. The effects of exit Mach number, exit Reynolds number, inlet boundary layer thickness, gas to wall temperature ratio, inlet pressure and temperature gradients were investigated. The effect of changing the coolant to mean gas flow rate ratio or the effect of coolant temperature did not investigated.

Localized injection of cooling air into the boundary layer along the surface is the technique employed in film cooling. The coolant injected into the mainstream can be considered as a heat sink for the heat flow from the mainstream or as an insulating layer between the mainstream and the blade surface. Because the coolant mixes with the mainstream, the film is not in general a very effective method of cooling by itself. However, film cooling used in combination with convection cooling can result in significant reductions in heat flux and thereby contributing to high overall cooling

effectiveness. Liess [13] reported heat transfer measurements for injection through a row of 35 degree holes with a lateral spacing of 3 diameters. He showed that close to the injection holes, the heat transfer coefficient increased by up to 60 percent above the non-injection value and further downstream, the increase was up to 25 percent. Using an injection geometry similar to that of Liess [13], Eriksen and Goldstein [14] showed at low blowing parameters that, the heat transfer coefficient with film injection was approximately equal to the heat transfer coefficient with no film injection. Metzger and Fletcher [15] explored the variation of the laterally averaged heat transfer coefficient downstream of a row of holes on a flat plate. Significant increase (up to 50 percent) in the heat transfer coefficient close to the injection holes for large blowing rates was found. Similar results for injection through two rows of staggered holes on the suction surface of turbine vanes and for injection on a flat surface were reported respectively by Lander *et. al.* [16] and Jabbari and Goldstein [17]. Camci [18] indicated in his study on rotor blades that, when only internal cooling is applied without external cooling, the leading edge is found to be the most critical area as far as the magnitude of local wall heat fluxes are concerned. However, the wall temperatures in this region are quite reduced to about 70 percent of those without cooling.

The effect of film cooling and mainstream turbulence on the leading edge heat transfer coefficient and film cooling effectiveness were experimentally investigated by Ou and Han [19, 20]. Their results showed that the leading edge heat transfer coefficient increases and film effectiveness decreases with increasing both the blowing ratio and the main turbulence level. However, the mainstream turbulence effect on the film effectiveness is reduced as the blowing ratio is increased.

The experimental investigation reported herein aims at studying the influence of internal cooling in case of variable surface temperature distribution on the aerodynamic flow characteristics and the heat transfer through the stationary blades of the first stage of gas turbines. The effect of internal cooling as well as the effect of inlet conditions of the main flow on blade surface temperature distribution, cooling effectiveness and heat transfer are investigated. In addition, the effects of coolant mass flow rate and inlet coolant temperature on these parameters are also examined. The velocity profiles in the boundary layer at the mid-span and at different locations along the suction surface are measured. The boundary layer parameters along the blade surface are calculated from the measured velocity distributions.

EXPERIMENTAL FACILITY

The apparatus on which the experimental program was conducted is shown schematically in Figure 1. It consists of a heating system, a convergent transition section, an instrumental inlet section, a cooling system and an instrumental cascade section.

The Heating System

The heating system is a gas fired burner consists of two concentric steel tubes. The outer tube is 208 mm inner diameter, 8 mm wall thickness and 1000 mm length. The inner one, Figure 2, is 107 mm inside diameter, 4 mm wall thickness and 800 mm length. The tube has 84 holes distributed symmetrically on its wall at fourteen stations. Air enters the burner continuously from an air source and is controlled by means of a valve. The air flow rate is measured by a calibrated orifice meter and it is admitted partially to the burner at three sections. The first part was admitted at the beginning of the burner through 48 mm inner diameter tube. This part of air was adjusted by a control valve to achieve the suitable air-fuel ratio for complete combustion. The second part was admitted at a forward section of the outer tube through 35 mm inner diameter steel tube. This part of air is important for decreasing the inner tube wall temperature and helps for good stability of flame and draughting of

the produced gases. The third part of air was by-passed after the burner to control the required gas temperature. The fuel was injected at the entry of the inner tube. Fuel injector, Figure 3, was made of brass and enclosed by a swirler to ensure good mixing of air and fuel. The swirler has two flat blades and was made of a steel sheet. The swirl angle is taken to be 45 degrees to ensure good mixing between air and fuel. A valve and pressure gauge were installed on the fuel line to control the suitable amount of fuel. The fuel was ignited by means of an electrical spark plug system installed inside the inner tube.

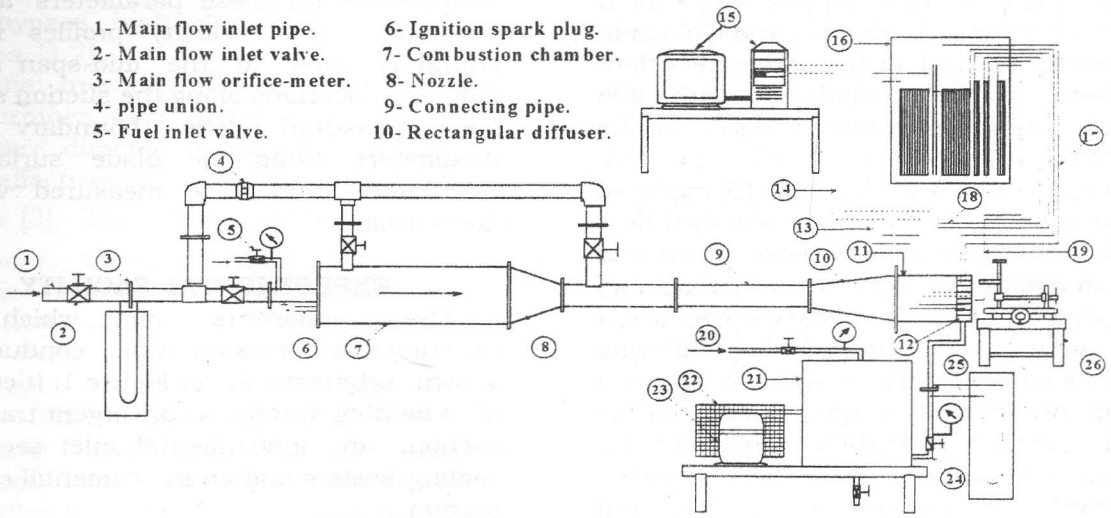

Figure 1 Schematic layout of the apparatus

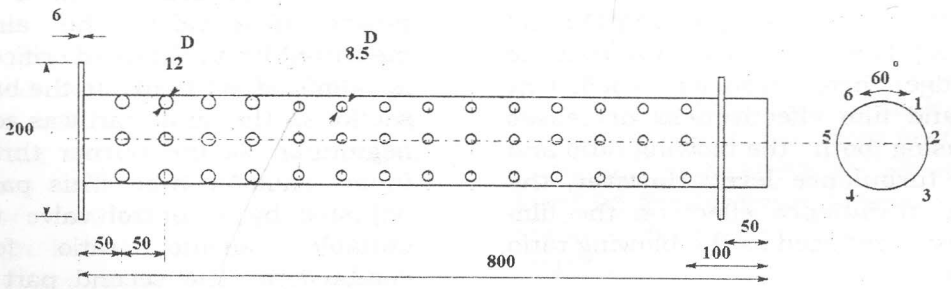

Figure 2 Inner tube of the burner, dimensions in mm.

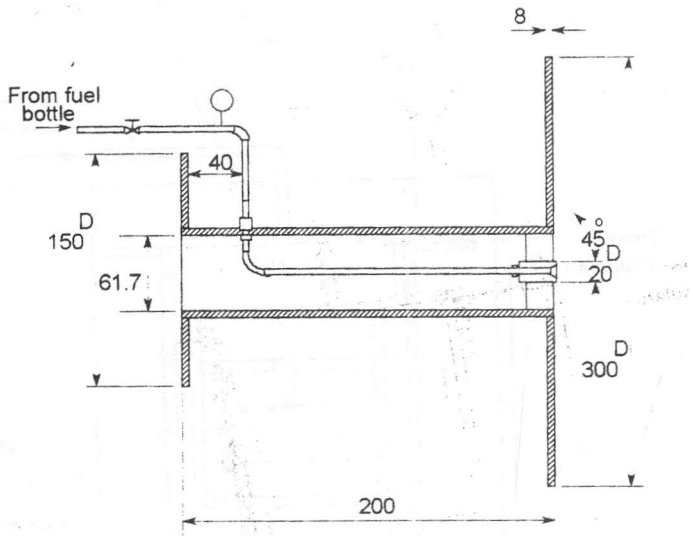

Figure 3 Fuel injector, dimensions in mm.

The Cooling System

A cooling unit was designed to cool the air required for cooling the blades. The unit consists, as shown in Figure 4, of a compressor, a condenser, a filter-dryer, an expansion device, an evaporator and a thermostat. The compressor used was hermetically sealed and of the reciprocating type. It consumes power of 200 watt. The evaporator unit is a finned coil supported inside a cylindrical steel tank 390 mm inner diameter, 12 mm wall thickness and 655 mm height. The tank has a circular cover 580 mm diameter and sealed with a rubber washer to prevent leakage. An air fan was installed inside the tank to produce swirling of air inside it to achieve good heat transfer between the air and the evaporator coil and also to ensure homogeneous temperature distribution in the air. The air required for cooling flows from the main supply line to the evaporator tank through 15.2 mm inner diameter steel tube. Cooled air flows from the tank to the test section through 15.2 mm inner diameter steel tube. The required coolant air was controlled with the aid of two valves before and after the tank and a calibrated orifice meter.

The Inlet Section

The inlet section (11) is a steel rectangular duct 400 mm in length and is 227×56 mm inlet cross sectional area. The inlet section has a fixed core and contains the total pressure and temperature probes and the wall static pressure tapes. The inlet conditions are measured in the constant-area inlet section at about four axial chords upstream of the blade cascade so as not to disturb the blades.

The Cascade Section

The test section (12) has a seven blades linear cascade, as shown in Figure 5, arranged at 30 degrees staggered angle. The blade profiles are representative of the first stage, stator gas turbine as shown in Figure 6. Specific geometric details are given in Reference 21.

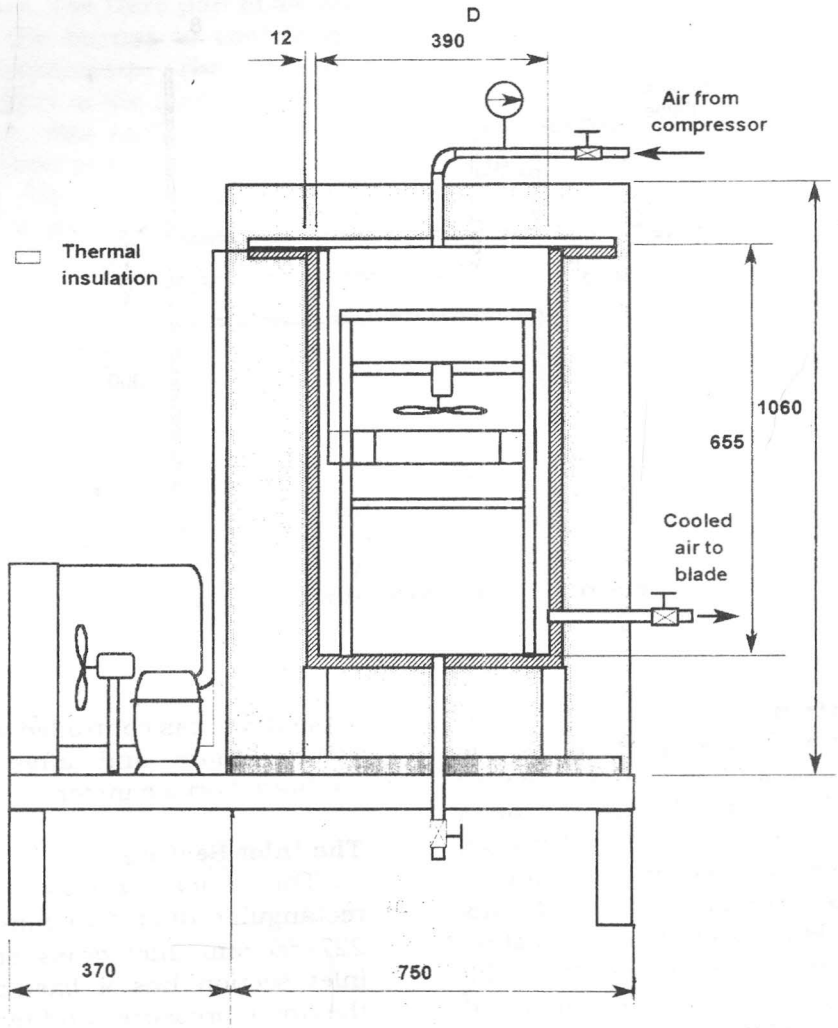

Figure 4 Cooling system, dimensions in mm.

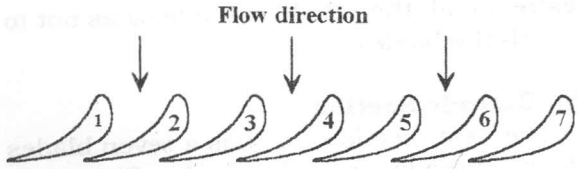

Figure 5 Cascade arrangement

The blades were fabricated of stainless steel and manufactured with an electric wire, computerized, cutting machine. The blades have arithmetic surface roughness (R_a) of 1.47 μm. The chord length (C) and the height (h) of the blade are respectively 51.46 and 56 mm. The inlet and outlet blade angles (β_1 and β_2) were respectively 90° and 15° measured from the axial direction. The cascade was fixed at the end of the inlet section. For blade cooling process, a hole of 4 mm diameter was drilled parallel to the blade height to form the coolant air flow passage. The position of the cooling passage was chosen to be at the largest thickness of the blade, near the leading edge, as shown in Figure 6.

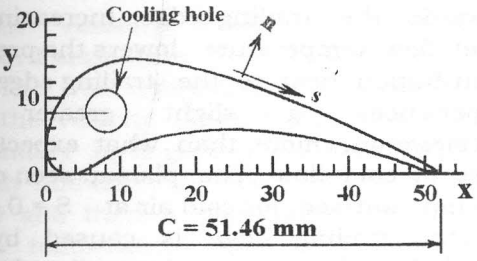

Measuring Locations

Point No.		1	2	3	4	5	6	7
S	(P-S.S.)	0.122	0.270	0.377	0.464	0.549	0.628	0.710
	(P-S.S.)	0.155	0.238	0.327	0.402	0.500	0.584	0.674
	(T-S.S.)	0.155	0.232	0.360	0.486	0.619	0.756	
	(T-S.S.)	0.155	0.316	0.464	0.614			

(P-S.S.) Measuring locations of static pressure on suction surface
(P-S.S.) Measuring locations of static pressure on pressure surface
(T-S.S.) Measuring locations of static pressure on suction surface
(T-S.S.) Measuring locations of static pressure on pressure surface

Figure 6 Cooling passage position

Experimental Measurements and Uncertainty

The total pressure was measured before the inlet to the cascade with the aid of a calibrated total-static Pitot tube to establish the total and static pressure at the cascade inlet. Blades 3 and 5 in the cascade arrangement have static pressure taps on the suction and pressure surfaces respectively, see Figure 5. A multi-tube water manometer was used for measuring the static pressure distribution. The experimental errors are calculated according to the technique represented in Reference[22]. The experimental error in measuring the static pressure was about ±0.1 percent.

The velocity distribution in the boundary layer was measured on the suction surface at four stations before the trailing edge at dimensionless surface distance (S) of 0.464, 0.549, 0.628 and 0.710. The measurements of velocity profiles were conducted for the cases of cold and hot gas flows with and without cooling. A flatted three hole probe was used for measuring the velocity profiles. The probe head was made from steel tubing of 0.7 mm outer diameter and 0.4 mm inner diameter. The probe was moved in the direction normal to the blade surface through steps of 0.2 mm near the blade surface. The step size was increased further out, giving about five points over the boundary layer thickness. The experimental error in measuring the velocity was about ±0.5 percent.

The temperature was measured before and after the cascade and along the pressure and suction surfaces of the blade with the aid of calibrated Nickel Chrome-Nickel Aluminum thermocouples of 0.5 mm diameter and insulated by high temperature synthetic fibers. The center blade of Figure 5 has thermocouples installed in grooves. The blade surface temperature distribution was measured along the blade surface at its mid-span. It was measured at four sections on the pressure surface and at six sections on the suction surface. The thermocouples were attached to a data acquisition system. The data acquisition system type NI-DAQ is supplied with SCXI-1000 interface capable of 32 channels. The accuracy of the data acquisition system is 0.01 percent. All of the temperature signals are acquired and sent to a personal computer for managing and plotting. The system permits temperature reading for all points at steady state at the same time. The experimental error in measuring the temperature was about ±1 percent.

Experimental Procedure

The experimental procedure involves measurements in the cases of cold air and hot gas flows with and without cooling for two main mass flow rates, namely 3.7 and 5.2 kg/min. The pressure and temperature distributions were measured in each case and the cooling effectiveness, heat transfer coefficient were calculated. For each case of gas flow rate, the temperature at cascade inlet was controlled at three values of 473, 493 and 513 K by controlling the fuel flow rate. The inlet coolant temperature was changed to have three values of 283, 288 and 293 K for each case of inlet gas temperature. It was controlled by the cooling unit thermostat. The experiments were conducted at three values of coolant mass flow rates, namely 0.009, 0.012 and 0.015 kg/min.

For conducting experiments in the steady state, the required amount of main flow was permitted to flow through the burner then fuel was injected and the spark was ignited. The hot gas produced by combustion is passed through a duct to the cascade. In case of no cooling of the blade, the temperature was observed at the computer monitor until it reaches a steady state (usually in 10-15 minutes) then all of the temperature readings are recorded at the same time for all points. Coolant was permitted to pass through the cooling passage at the required coolant temperature and its required mass flow rate tests were recorded when the steady state was reached. The tests were repeated at different coolant mass flow rates and different inlet coolant temperatures. Furthermore, the previous experimental tests were repeated for different inlet gas temperature and different hot gas flow rate.

RESULTS AND DISCUSSION

The results are represented graphically in order to indicate the effect of heating and cooling on fluid flow characteristics, cooling effectiveness and the variation of heat transfer coefficient along blade surfaces for various cases.

Static Pressure distributions

The static pressure distribution along the blade pressure and suction surfaces is plotted in Figure 7 for cold and hot gas flows at a rate of 3.7 kg/min. The absolute inlet temperature of cold air is 293 K while that of hot gas is selected as 473, 493 and 513 K. The corresponding exit Reynolds number of the previous main flow temperatures are $3.09X10^4$, $2.07X10^4$, $2.47\ X10^4$ and $2.54\ X10^4$ respectively. It is observed clearly from this figure that the pressure distribution for the hot gas flow takes the same trend as in the case of cold flow. However, on the pressure surface, the pressure increases with increasing the inlet temperature of the main flow. The pressure distribution along the suction surface illustrates that, the static pressure decreases continuously along the suction surface as the flow moves towards the trailing edge. Increasing the inlet flow temperature lowers the pressure distribution near to the trailing edge. This experiences a slight greater flow acceleration, more than what expected in case of cold flow. The plateau seen on the suction surface for cold air at S = 0.45 up to the trailing edge is caused by the possibility of separation. Increasing the inlet flow temperature shifts this possibility towards the trailing edge.

The Reynolds number increase with rising the inlet gas temperature is due to increasing the gas velocity. The influence of Reynolds number level is reflected in the transitional behavior along the suction surface as well as in the general level of surface heat transfer. It is observed from Figure 7 that, increasing the exit Reynolds number causes an increase of static pressure along both suction and pressure surfaces.

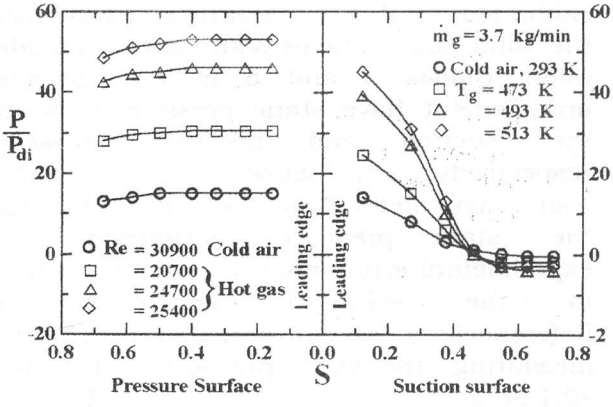

Figure 7 Effect of heating on the static pressure distribution

However, increasing the Reynolds number causes the pressure variation on the suction surface experiences strongly favourable pressure gradient. The effect of favourable pressure gradient is to suppress turbulence in the boundary layer whereas the effect of adverse pressure gradient is to increase turbulence intensity [23]. The influence of Reynolds number on heat transfer distribution is reflected in the transitional behavior along the suction surface as will be discussed later.

Mean Velocity Profiles and Boundary Layer Parameters

The wall temperature has a great effect on the velocity profiles and hence on the boundary layer growth and heat transfer. To study this effect the blade was heated by gas flow and then it was cooled while the inlet gas temperature was kept constant. A sample of the experimental results which are obtained for inlet gas and coolant temperatures of 473 and 293 K respectively are presented. The measured velocity profiles along the suction surface are shown in Figure 8 for cold air and hot gas flows in both cases of blade with and without cooling. The profiles are plotted in the wall regions for indicating the effects of heating and cooling. The effect of cooling on the first measured velocity profile at S = 0.464, Figure (8-a), is remarkable to increase the velocity values compared to that of uncooled blade surface. Unfortunately, the difference in velocity values appear to be small due to the limited coolant mass flow ratio ($\dot{m}_c / \dot{m}_g$) which is admitted to the cooling passage. In addition, the effect of cooling on the velocity profiles disappeared as the flow approaches the cascade exit. This is because the cross section area of the cooling passage is small and limited with the maximum blade thickness. If the cooling is applied for a hollow blade, the influence of cooling becomes more effective on the flow characteristics across the blade passage. The integral boundary layer parameters which are known as the boundary layer thickness (δ), displacement thickness (δ^*), the momentum thickness (θ) and the shape factor (H) are calculated from the measured mean velocity profiles for the different cases. The displacement thickness and the momentum thickness in all figures are normalized by the boundary layer thickness (δ). Figure 9 illustrates the effect of heating and cooling on the growth of the boundary layer parameters. For cold air flow case, the displacement and momentum thickness increase with increasing the distance (S) along the blade surface. Correspondingly, the shape factor of the boundary layer increases with increasing the distance (S) as shown in Figure 9-c. It is also noticed that, the values of the shape factor at about S = 0.7 and near the trailing edge does not reach the separation criterion, which is taken as $1.8 < H < 2.4$ [24]. In the case of hot gas flow without cooling, it is clearly shown that the displacement and the momentum thicknesses as well as the shape factor of hot gas flow have values smaller than those of cold air flow case. Therefore, the effect of blade cooling is understood to increase the values of displacement and momentum thicknesses compared with that of heated blade without cooling. To summarize, the blade cooling has a destabilizing effect on the boundary layer development along the blade suction surface. As a consequence, the destabilizing effect of the boundary layer which means that an increase of the boundary layer thickness will reduce the rate of heat transfer between the flow gases and the blade wall; this will be discussed later.

Variation of Wall-to-Gas Temperature Ratio

The ratio of wall-to-gas temperature (T_w / T_g) of gas turbine blades is an important parameter as it indicates the rate of heat transfer around the blade surface. It is influenced by many parameters such as inlet gas temperature, coolant inlet temperature, coolant and gas flow rates. Figures 10 and 11 indicate the effect of cooling on the distribution of the wall-to-gas temperature ratio. The main flow rate of the hot gas is taken as 3.7 kg/min and its inlet temperature is 473 K. In Figure 10 the coolant temperature is kept constant at 293 K while the coolant flow ratio ($\dot{m}_c / \dot{m}_g$) was chosen to be 2.432×10^{-3}, 3.243×10^{-3} and 4.054×10^{-3}.

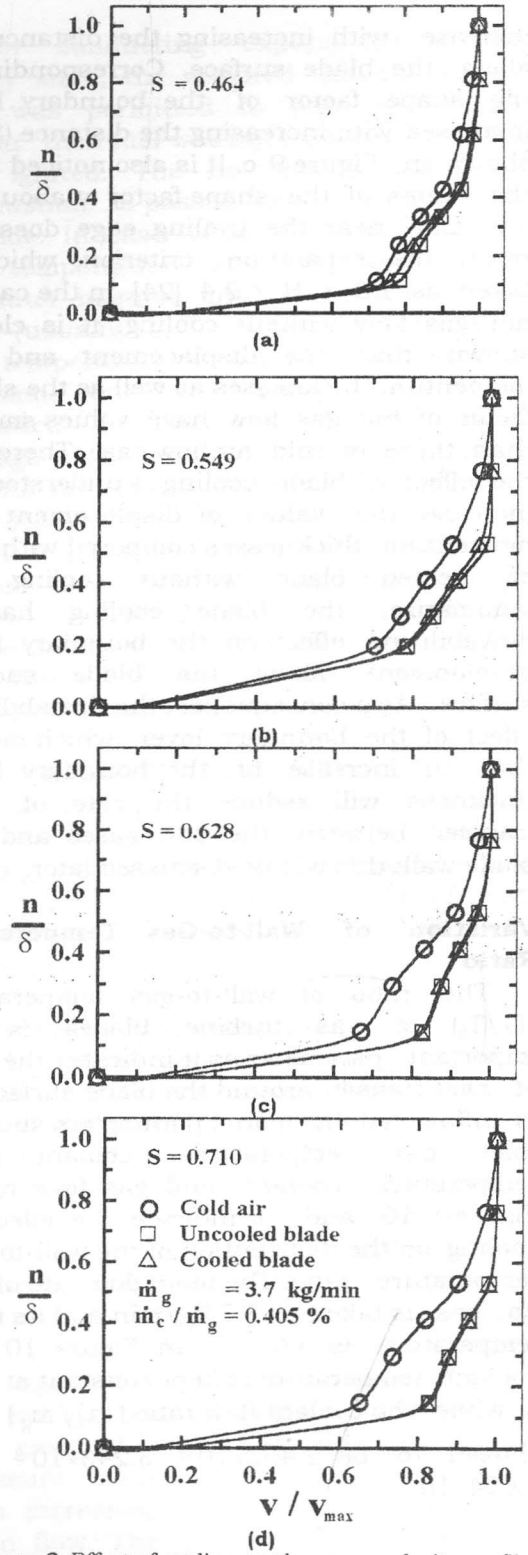

Figure 8 Effect of cooling on the mean velocity profile on the suction surface

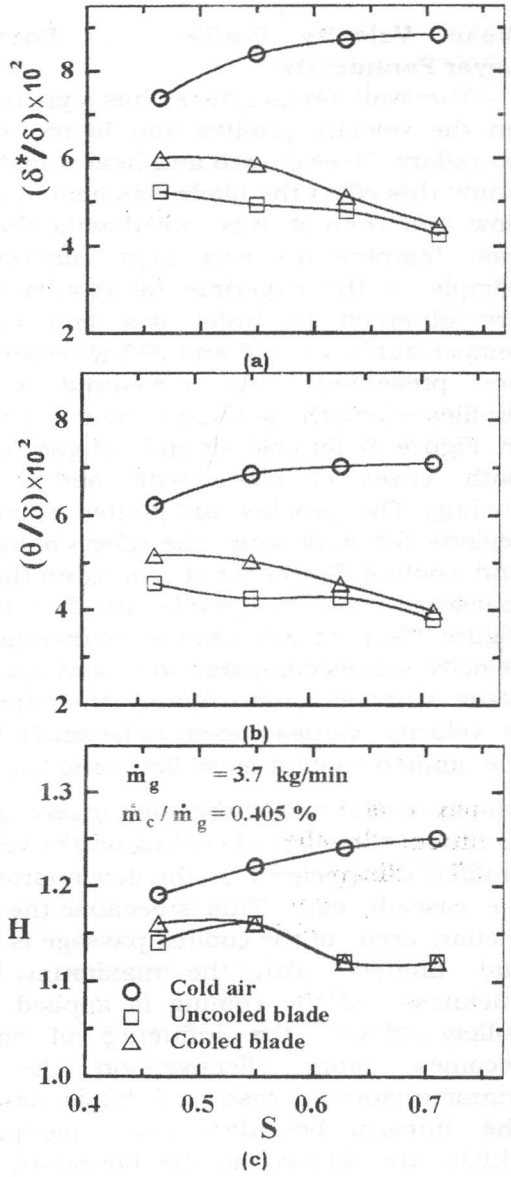

Figure 9 Effect of cooling on the boundary layer parameters

For cooled blade, it appears in this figure that, the wall-to-gas temperature decreases on the pressure surface up to S about 0.32 of the arc length where it reaches its lower value then it increases again. On the suction surface, this ratio decreases in the region close to the leading edge and then increases towards the blade trailing edge. For constant ratio of coolant-to-gas temperature, the wall-to-gas temperature

ratio decreases on both surfaces of the blade with increasing the ratio of coolant mass flow rate. This may be due to the occurrence of transition and turbulent boundary layer very near to the leading edge which increases the boundary layer thickness and hence the turbulent heat transfer rate becomes small. It is also observed that the rate of increase of T_w/T_g increases with increasing the coolant mass flow rate ratio as the flow approaches the trailing edge. This is because of the effect of vanishing of the cooling as the flow moves downstream the cascade. In Figure 11, the coolant temperature was changed to be 283, 288 and 293 K while the coolant mass flow ratio was kept constant at 0.405%. It is observed clearly that, the wall-to-gas temperature ratio (T_w /T_g) decreases when the inlet coolant temperature is decreased. This is attributed to the increase in temperature difference between the cooling passage and the blade surface exposed to the hot gas flow which leads to a decrease in the wall temperature. Consequently, a decrease in the wall temperature causes an increase in the boundary layer thickness which increases in turn the thermal resistance and reduces the heat transfer process.

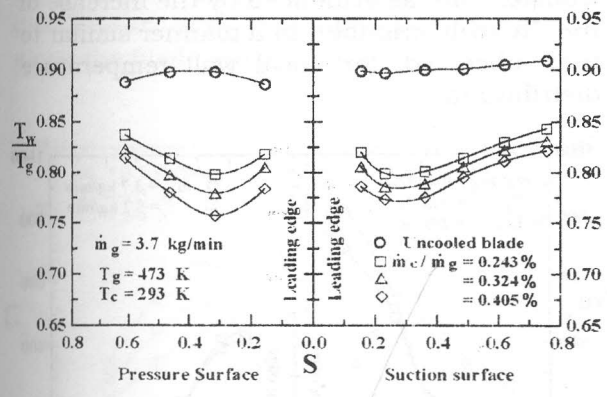

Figure 10 Effect of coolant mass flow ratio on the distribution of T_w/T_g

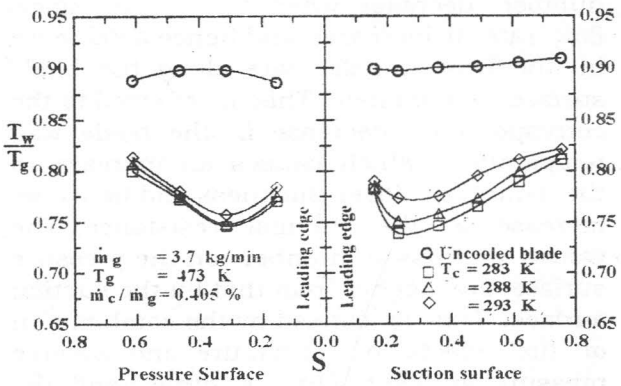

Figure 11 Effect of coolant inlet temperature on the distribution of T_w/T_g

Variation of the Heat Transfer Coefficient

At steady state heat transfer, the local heat transfer coefficient (α_g) is evaluated with the following equation, neglecting the heat loss,

$$\dot{Q} = \alpha_g A_s (T_g - T_w) = -k A_n \frac{\partial T}{\partial n} \qquad (1)$$

where $\dot{Q}$ is the rate of heat transferred. T_g and T_w are the local gas temperature and the local blade wall temperature, k is the blade material thermal conductivity and A_s is the surface area which is calculated as A_s = s h. Where s and h are the distances along the blade surface measured from the leading edge and the blade height, recpectively. A_n is the normal area of heat conduction and $\partial T/\partial n$ is the temperature gradient in the normal direction. The local Nusselt number can be calculated with knowing the local gas heat convective coefficient as follows:

$$Nu_x = \alpha_g s / k_g \qquad (2)$$

where k_g is the gas thermal conductivity.

Figure 12 illustrates the effect of coolant mass flow rate on the distribution of local Nusselt number along the pressure and suction blade surfaces. The results are plotted for 3.7 kg/min hot gas flow rate at gas inlet temperature of 513 K and at coolant inlet temperature of 293 K. As shown from this figure, the values of Nusselt

number decrease when the coolant mass flow rate is increased and hence a decrease in the heat transfer rate along the blade surface is obtained. This is referred to the corresponding decrease in the blade wall temperature which causes an increase in the boundary layer thickness and hence an increase in the thermal resistance. The values of Nusselt number on the pressure surface are higher than that on the suction surface. This is caused by the combination of the effects of curvature and adverse pressure gradient. On the other hand, the Nusselt number has a higher value near the leading edge where it experiences the stagnation values with very thin boundary layer thickness. On the pressure surface, the Nusselt number decreases rapidly in the direction of trailing edge until about 45 percent of the blade arc then the rate of decrease is lowered.

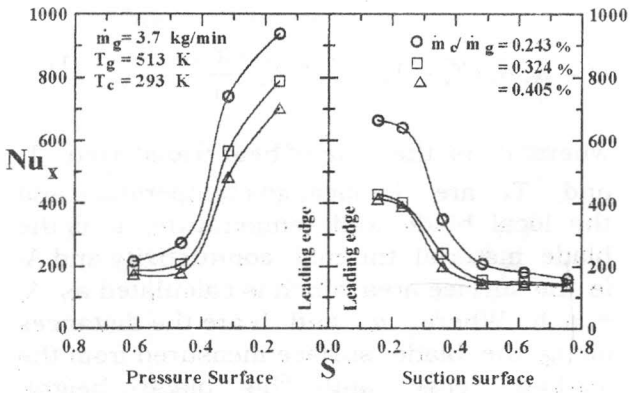

Figure 12 Effect of coolant flow rate on Nusselt number distributions

On the suction surface, the Nusselt number decreases steeply until about 40 percent of the blade arc and then the rate of decrease is lowered.

Figure 13 presents the effect of gas inlet temperature on the distribution of Nusselt number at the same coolant mass flow rate and constant coolant inlet temperature. Generally, the same distribution of the Nusselt number is observed. It appears that, the local Nusselt number increases on both surfaces of the blade with increasing the inlet gas temperature. This occurs due to the reduction of the boundary layer thickness when the gas temperature increases and consequently the heat transfer increases.

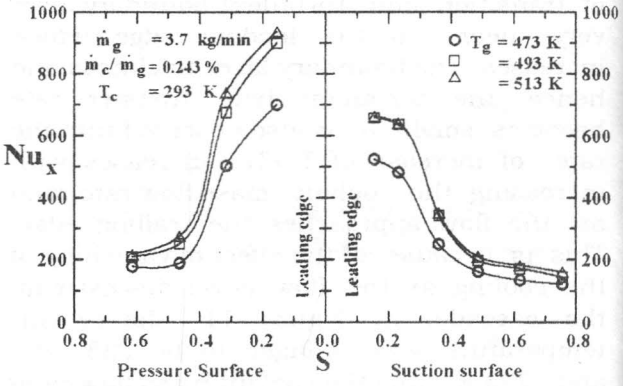

Figure 13 Effect of inlet gas temperature on Nusselt number distributions

The effect of increasing the mainstream flow rate, which means an increase in Reynolds number, on the variation of Nusselt number along the blade surfaces is presented in Figure 14 for inlet temperature of mainstream T_g = 513 K. The coolant mass flow rate and its temperature are kept constant at 0.015 kg/min ($\dot{m}_c/\dot{m}_g$ = 0.405%) and 293 K, respectively. It is seen from this figure that, the influence of increasing the mainstream flow rate or the Reynolds number is to increase the heat transfer rate as evidenced by the increase of the Nusselt number, in a manner similar to that observed for local wall temperature distributions.

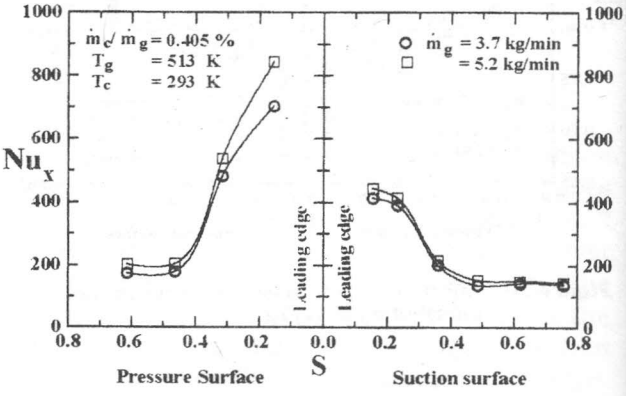

Figure14 Effect of inlet gas flow rate on Nusselt number distributions

Variation of Cooling Effectiveness of the Blade

The cooling performance of gas turbine blades is expressed in the form of cooling effectiveness. Masaru *et al.* [25] defined the cooling effectiveness (ε_x) as:

$$\varepsilon_x = \frac{T_g - T_w}{T_g - T_c} \qquad (3)$$

Figure 15 indicates the axial variation of the cooling effectiveness at different coolant mass flow rates and constant hot gas. The inlet gas and coolant temperatures are respectively 473 and 293 K. It is indicated that, the local cooling effectiveness at the leading edge is small because it is exposed to the highest heat fluxes resulting from the very thin boundary layer thickness at this section. On the suction surface, the maximum cooling effectiveness was achieved near the blade leading edge then it decreases towards the trailing edge. On the pressure surface, the blade cooling effectiveness reaches its maximum value at 32 percent of the blade surface arc, then it decreases again. There is a remarkable improvement of the cooling effectiveness with increasing the coolant mass flow rate. This is due to the decrease of the wall temperature which results in a poor distribution of the boundary layer thickness along the blade surface.

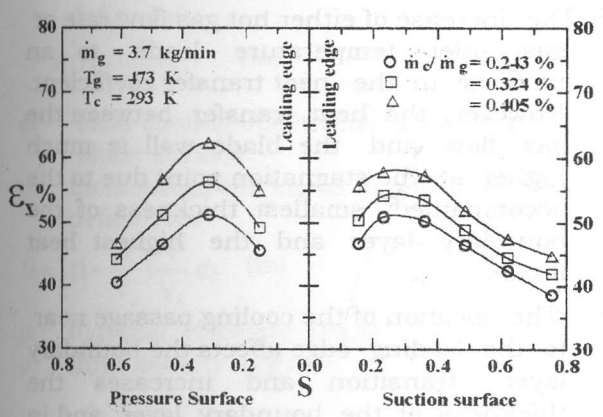

Figure 15 Effect of coolant flow rate on the cooling effectiveness

The average cooling effectiveness (ε_{av}) can be calculated from the following equation [25]:

$$\varepsilon_{av} = \frac{T_{g,m} - T_{w,m}}{T_{g,m} - T_c} \qquad (4)$$

where $T_{g,m}$ is the mean gas temperature between inlet and outlet of the cascade, $T_{w,m}$ is the wall mean temperature and T_c is the coolant inlet temperature. Figure 16 indicates the effect of the coolant mass flow ratio ($\dot{m}_c/\dot{m}_g$) on the average cooling effectiveness (ε_{av}) for mainstream flow rate of 3.7 kg/min. In Figure 16-a, the inlet gas temperature is kept constant at 473 K while the coolant inlet temperatures are taken to be 283, 288 and 293 K. It is observed that the average cooling effectiveness increases, as expected, with increasing the coolant mass flow ratio. This is referred to the accompanied decrease of the blade wall temperature with increasing the coolant mass flow rate which leads to an increase in the heat transfer between the coolant passage and the blade surface and consequently decreases the blade wall temperature. It is seen also that the mean cooling effectiveness increases when the coolant inlet temperature decreases. In Figure 16-b, the results of the average cooling effectiveness are plotted against the coolant mass flow ratio at constant coolant inlet temperature (T_c = 283 K) while the inlet gas temperatures are taken to be 473, 493 and 513 K respectively. It is clearly observed that, the mean cooling effectiveness of the blade decreases with increasing the gas inlet temperature. This is referred to that, increasing the gas inlet temperature at constant coolant temperature and coolant flow rate tends to increase the temperature difference between the gas and the coolant which becomes higher than the temperature difference between the gas and the blade surface temperature.

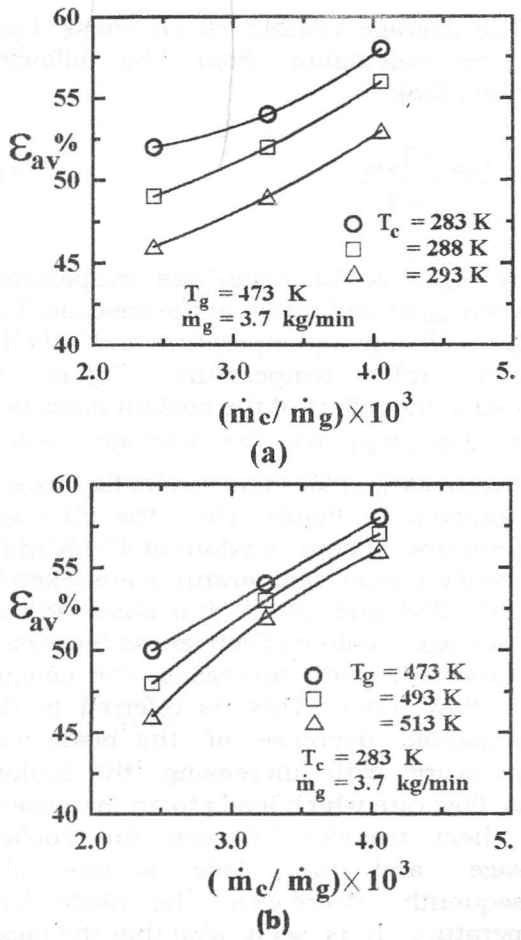

Figure 16 Effect of coolant and gas inlet temperatures on the average cooling effectiveness

This reduces the average blade cooling effectiveness. However, the rate of increase of the mean cooling effectiveness increases at higher inlet gas temperature compared with that at lower gas inlet temperature. It appears from this figure that, if the coolant mass flow rate is increased, the mean cooling effectiveness (ε_{av}) may have the same final value for all tested inlet gas temperature. This is referred to the increase of the wall temperature and the high temperature gradient due to the rise of gas inlet temperature.

CONCLUSIONS

The effect of internal cooling on the areodynamic flow characteristics and the heat transfer through the stationary blades of the gas turbine has been investigated experimentally. The following conclusions can be drawn:

1. The cooling of the blade in case of variable surface temperature distribution causes substantial increase in the values of displacement and momentum thicknesses of the boundary layer compared to uncooled blade.
2. The blade wall-to-gas temperature ratio is affected by many parameters such as mainstream flow rate, inlet gas temperature, coolant mass flow ratio and coolant inlet temperature. It increases with increasing either mainstream flow rate or the inlet gas temperature while the increase of coolant mass flow rate leads to a decrease in the wall-to-gas temperature ratio. The decrease of coolant inlet temperature results in decreasing the blade wall-to-gas temperature ratio as a result of the increase in the temperature difference between the cooling passage and the blade exposed surface to the hot gas flow.
3. The leading edge is the most critical area exposed to heat transfer which causes higher gas-to-wall temperature ratio.
4. The cooling effectiveness of the blade increases with increasing the coolant mass flow ratio. The blade cooling can result in a significant reduction in heat flux and thereby contributing to high overall cooling effectiveness.
5. The increase of either hot gas flow rate or gas inlet temperature leads to an increase in the heat transfer coefficient. However, the heat transfer between the gas flow and the blade wall is much higher at the stagnation point due to the accompanied smallest thickness of the boundary layer and the highest heat fluxes.
6. The location of the cooling passage near to the leading edge affects the boundary layer transition and increases the thickness of the boundary layer and in turn causes a more reduction in the heat transfer coefficient.

NOMENCLATURE

A blade surface area (m^2)
C blade chord (m)
Cp specific heat (kJ/kg.K)
D cooling passage diameter (m)
H shape factor (δ^*/θ)
h blade height (m)
k blade material thermal conductivity (W/m K)
k_g the gas thermal conductivity (W/m K)
L_s blade surface length (m)
$\dot{m}$ mass flow rate (kg/s)
n normal distance measured from the blade surface (m)
Nu_x local Nusselt number (α_g s / k_g)
P static pressure (bar)
P_{di} inlet dynamic pressure (bar)
$\dot{Q}$ heat transfer rate (W)
Re Reynolds number based on the exit conditions ($\rho VC/\mu$)
s distance along the blade surface measured from the leading edge (m)
S dimensionless distance along the blade surface (s/L_s)
T temperature (K)
V local velocity (m/s)
x, y axial and normal cartesian coordinates
α_g local convective heat transfer coefficient (W/m^2K)
β_1 blade inlet angle (degrees)
β_2 blade outlet angle (degrees)
δ boundary layer thickness (m)
δ^* boundary layer displacement thickness defined as:

$$\delta^* = \int_0^{\delta} (1 - \frac{V}{V_e}).dy \quad (m)$$

ε_x local cooling effectiveness along the blade surface
θ momentum thickness of boundary layer defined as:

$$\theta = \int_0^{\delta} (1 - \frac{V}{V_e}) \frac{V}{V_e}.dy \quad (m)$$

μ dynamic viscosity (Pa.s)
ρ fluid density (kg/m^3)

Subscripts

a air
av average
c coolant
di dynamic at inlet
e boundary layer edge
g gas
i inlet
max maximum condition
n normal to blade surface
s along the blade surface
w wall

REFERENCES

1. G. L. Wilde, "The Design and Performance of High Temperature Turbines in Turbofans Engines," Aeronautical Journal, No. 600, pp. 342-352, (1977).
2. O. N. Favorskll, and S. Z. kopelev, "Air Cooling of Gas Turbine Blades," Thermal Engineering, No. 28, pp. 435-438, (1981).
3. J. G. Reuter, C. Gazley, "Computed Temperature Distribution and Cooling of Solid gas Turbine blades," NACA RME 7B11g, (1947).
4. W. Byron Brown, and J. N. B. Livingood, "Cooling Effects from Use of Ceramic Coatings on Water Cooled Turbine Blades," NACA RM E8H03, (1948).
5. F. J. Hartwig, W. B. Brown and J. N. B. Livingood, "Preliminary Investigation of a Gas Turbine with Sillimanite Ceramic Rotor Blades," NACA TN 1398, (1947).
6. J. N. B. Livingood, H. H. Ellerbrock and F. J. Hartwig, "Analysis of Spanwise Temperature Distribution in Three Types of Air Cooled Turbine Blades," NACA Report 994, (1950).
7. J. M. Hannis, and M. K. D. Smith, "The Design and Testing of Air Cooled Blading for an Industrial Gas Turbine," TRANS. ASME J. Engineering for Power, Vol. 105, pp. 466-473, (1983).
8. S. R. Kennon, and G. S. Dulikravich, "The Inverse Design of Internally Cooled Turbine Blades," TRANS. ASME, J. Engineering for Gas Turbine and Power, Vol. 107, pp. 123-126, (1985).
9. L. D. Daniels, and W. B. Brown, "Calculation of Heat Transfer Rates to Gas Turbine Blades", Int. J. Heat and

Mass Transfer, Vol. 24, No. 5, pp. 871-878, (1981).
10. L. A. Walker, E. and Markland, " Heat Transfer to Turbine Blading in the Presence of Secondary Flow," Int. J. Heat and Mass Transfer, Vol. 8, pp. 729- 748, (1965)
11. V. M. Kapinos, and Sletenko, "Determination of Average Coefficients of Heat Transfer from Turbine Blades," Thermal Engineering, Vol. 28 No. 8, pp. 458-460, (1981).
12. R.E. York, L.D. Hylton, and M.S. Mihelc, "An Experimental Investigation of End Wall Heat Transfer and Aerodynamics in a Linear Vane Cascade," TRANS. ASME, J. Engineering for Gas Turbines and Power, Vol. 106, pp. 159-167, (1984).
13. C. Liess, "Experimental Investigation of Film Cooling with Ejection from a Row of Holes for the Application to Gas Turbine Blades," TRANS. ASME, J. Engineering for Power, Vol. 97, pp. 21-27, (1975).
14. V. L. Eriksen, and R. J. Goldstein, "Heat Transfer and Film Cooling Following Injection Through Inclined Circular Holes," ASME, J. Heat Transfer, Vol. 96, pp. 239-245, (1974).
15. D. E. Metzger, and D. D. Fletcher, "Evaluation of Heat Transfer for Film Cooled Turbine Components." J. Aircraft, Vol. 8, No. 1, pp. 33-38, (1971).
16. R. D. Lander, R.W. Fish, and M., Suo, "External Heat Transfer Distribution on Film Cooled Turbine Vanes," J. Aircraft, Vol. 9, No. 10, pp. 707-714, (1972).
17. M. Y. Jabbari, and R. J. Goldstein, "Adiabatic Wall Temperature and Heat Transfer Downstream of Injection Through Two Rows of Holes," TRANS. ASME, J. Engineering for Power, Vol. 100, pp. 303-307, (1978).
18. C. Camci, "An Experimental and Numerical Investigation of Near Cooling Hole Heat on a Film-Cooled Turbine Blade," TRANS. ASME, J. Turbomachinery, Vol. 111, pp. 63-70, 1989.
19. S. Ou, and J. C. Han, "Influence of Mainstream Turbulence on Leading Edge Film Cooling Heat Transfer Through Two Rows of Inclined Film Slots," ASME, J. Turbomachenery, Vol. 114, pp. 724-733, (1992).
20. S. Ou, and J. C. Han, "Leading Edge Film Cooling Heat Transfer Through One Row of Inclined Film Slots Including Mainstream Turbulence Effects," J. Heat Transfer, Vol. 116, pp. 561-569, (1994).
21. M. E. Ditch, G. A. Phelepof, and L. I. Lazaref, "Atlas for Profiles of Axial Turbine Blades," Machine Building, (1965).
22. S. J. Kline, and F. A. McClintack, "Describing the Uncertainties in Single-Sample Experiments," ASME, Mechanical Engineering Journal, Vol. 75, pp. 3- 8, (1953).
23. A. Brown, and R. C. Burton, "The Effects of Free Stream Turbulence Intensity and Velocity Distribution on Heat Transfer to Curved Surfaces," TRANS. ASME. J. Engineering for Power, Vol. 100, pp. 159-168, (1978)
24. H. Schlichting, "Boundary Layer Theory," McGraw Hill Book Company, New York, (1968).
25. Masaru Hirata, Nobuhide Kasagi and Masaya Kumada, "Studies of Full-Coverage Film Cooling," Heat Transfer in Energy Problems, Hemisphere Publishing Corporation, (1979).

Received July 7. 1999
Accepted September 23. 1999

Cooling Effects on Boundary Layer Growth and Heat Transfer in Gas Turbine Blading Cascade

تأثير التبريد على نمو الطبقة المتاخمة وانتقال الحرارة في مصفوفه ريش توربينة غازية

حسن عوض عبد الله ، محمد خليل بسيونى، طاهر إبراهيم صبرى
و مصطفى أحمد عبد الباقى

قسم هندسة القوى الميكانيكية – جامعة المنوفية

ملخص البحث

فى هذا البحث تم إجراء دراسة معملية لتأثير التبريد الداخلى فى ريش التوربينات الغازية على نمو الطبقة المتاخمة وإنتقال الحرارة خلال الريشة. لإجراء هذه الدراسة تم تصنيع مصفوفة ريش خطية مكونة من سبع ريش من الصلب، كل ريشة لها بروفيل ريشة توجيه المرحلة الأولى للتربينة الغازية. تم تصنيع حارق لتسخين الهواء لدرجات حرارة عالية كذلك تم إجراء التبريد للريشة من خلال مجرى أنبوبى بالقرب من حافة المقدمة للريشة. تم تصنيع منظومة تبريد بغرض خفض درجة حرارة الهواء المستخدم فى تبريد الريشة. أجريت القياسات المعملية لكل من الضغط الإستاتيكى على سطحى الريشة، توزيع السرعة، درجة الحرارة. تم الحصول على خصائص الطبقة الجدارية من توزيع السرعة وخصائص إنتقال الحرارة للريشة من توزيع درجات الحرارة. أجريت التجارب المعملية للريشة الساخنة بدون تبريد وتحت ظروف التبريد المختلفة. كذلك أجريت التجارب المعملية لسريان الهواء تحت الظروف المعملية للحصول على الخصائص الإيروديناميكية لمصفوفة الريش.

أوضحت النتائج المعملية أن التبريد يزيد من سمك الطبقة الجدارية ويؤثر على تحول السريان الرقائقى إلى إضطرابى. وقد تبين من الدراسة أن رقم ناسلت يزداد عند إنخفاض معدلات مرور الهواء البارد وكذلك عند إرتفاع درجة حرارة الغازات أو زيادة معدلات تدفق الغازات (رقم رينولدز). وقد تبين أيضا أن الأداء التبريدى للريشة يزداد بزيادة معدلات مرور الهواء البارد ويقل بإرتفاع درجة حرارة الغازات أو زيادة معدل تصرفها.